

## **Bending tests of nail laminated timber (NLT): From the lamination to the composite panel**

Wei FENG<sup>a</sup>, Minjuan HE, Hengkun CAI<sup>a</sup>, Zheng LI\*

\*Department of Structural Engineering, Tongji University, Shanghai, 200092, China  
State Key Laboratory of Disaster Reduction in Civil Engineering, Tongji University, Shanghai, 200092, China  
A703, Civil Engineering Building, NO.1239 Siping Rd, Shanghai, China  
zhengli@tongji.edu.cn

<sup>a</sup> Department of Structural Engineering, Tongji University, Shanghai, 200092, China

### **Abstract**

Wood material is getting popular in spatial structures due to its natural renewability, distinctive aesthetic and good seismic performance. By nailing the wood laminations together through the wide faces, an engineered wood product called nail laminated timber (NLT) can be simply fabricated, which can serve as the alternative of the traditional glued laminated timber (Glulam) due to the advantages of good mechanical performance and low cost. In this study, the spruce-pine-fir dimension lumber was used as the lamination to fabricate the NLT panel. Then, to further improve the bending performance of NLT, the concrete was sheathed at the top of NLT to form the NLT-concrete composite (NLTCC) panel. Bending tests were conducted on the lamination, the NLT panel and the NLTCC panel, respectively. The failure modes and the bending properties of the specimens were analyzed. Finally,  $\gamma$ -method was used to predict the bending performance of the NLTCC panel. Results showed that NLT had more reliable performance than the lamination. The 5th percentile bending strength of the NLT could be 42.9% higher than that of the lamination. Compared to the NLT panel, the moment-resisting capacity (MRC) and the bending stiffness of the NLTCC panel improved by 38.3% and 78.2%, respectively.  $\gamma$ -method overestimated the MRC of the NLTCC panel by 11.3% but underestimated its bending stiffness by 4.7%, respectively.

**Keywords:** nail laminated timber, wood lamination, timber-concrete composite panel, bending test,  $\gamma$ -method

### **1. Introduction**

Wood material is getting popular due to its natural renewability, distinctive aesthetic and good mechanical performance [1]. The development of wood material in engineering, known as engineered wood products (EWPs), motivates its utilization in the large-span and the spatial structures [2]. Nail laminated timber (NLT) is also one of the EWPs, which is fabricated by nailing the wood laminations together along the wide faces. Due to the good mechanical performance and relatively low cost of NLT, it has the potential to serve as the alternative of the traditional glued laminated timber (Glulam) [3-5]. Nowadays, NLT is mainly used as the panel-type components, but there has been limited investigation into the design of NLT panels.

Recent research on NLT mainly focused on the experiment aspect to study its bending performance. For example, Taoum et al. [6] tested the bending performance of a locally post-tensioned NLT fabricated with radiata pine. Derikvand et al. [4, 7] tested the short-term and the long-term bending performance of NLT fabricated with fast-grown Eucalyptus. Herberg [8] tested the bending performance of the butt-jointed NLT fabricated with northern red oak. As a repetitive-member assembly, the system effect might exist in NLT, rendering a higher design bending strength. However, the limited sample size, which was

less than three in these tests, makes it challenging to analyze the characteristic values of the bending properties of NLT.

The mechanical performance of the timber panels can be further improved by adding the concrete topping with the shear connectors, which is known as the timber-concrete composite panel. For NLT, the similar reinforcement can be adopted to fabricate the NLT-concrete composite (NLTCC) panel. Hong [9] tested the bending performance of the NLTCC panels with four kinds of truss plates as shear connectors. Results showed that the moment-resisting capacity (MRC) of the NLTCC panels reached 5 to 7 times the serviceability requirements. The  $\gamma$ -method slightly underestimated the bending stiffness, but greatly underestimated the MRC of the panel by up to 76%. Derikvand et al. [4] tested the bending performance of the NLTCC panels with 45° inclined crossing screws as shear connectors. Results showed that the use of concrete resulted in a 259% increase in stiffness and a 26% increase in MRC on average compared with the NLT panels. All the NLTCC panels were still in the linear-elastic range under the ultimate limit stage requirement.

It is shown that NLT has the potential for the construction of the floor and roof system, but the design and the property prediction of the NLT and the NLTCC panels still need further investigation. Therefore, in this study, a comparative study was conducted on the bending performance of the lamination, the NLT panel and the NLTCC panel based on the bending tests. The failure modes and the bending properties of the specimens were analyzed. Furthermore,  $\gamma$ -method was employed to predict the bending performance of the NLTCC panel.

## 2. Experimental method

### 2.1. Materials

Visually graded No. 2 spruce-pine-fir (SPF) dimension lumber, with the section size of 38 mm × 140 mm (width × height), was used as the laminations. The density of the lumber is 445 kg/m<sup>3</sup> on average with the coefficient of variation (COV) of 12.6%. The moisture content of the lumber is 10.8% on average with the COV of 13.2%. The APA19/32 grade oriented strand board (OSB) was sheathed on the top surface of the NLT specimens as a constructional measure, with the thickness of 11.1 mm.

The smooth shank paper-taped strip steel nails were used to connect the laminations. The diameter and the length of the nails were 3.3 mm and 83 mm, respectively. The full-threaded self-tapping screws (STs) with cylindrical heads were used as the shear connectors between the NLT and the concrete layer. The nominal diameter and the fully thread length of the STs were 7.0 mm and 240 mm, respectively.

The concrete designed with the grade of C35 [10] was casted in site for the NLTCC panel. The plain round bars with the grade of HPB 300 [11] were used as the constructional steel rebar grids at the bottom of the concrete layer. The diameter of the bars was 6.0 mm.

### 2.2. Specimen design

The lamination specimens are the dimension lumber with the section size of 38 mm × 140 mm and the total length of 3050 mm. 50 replicates were designed for the lamination.

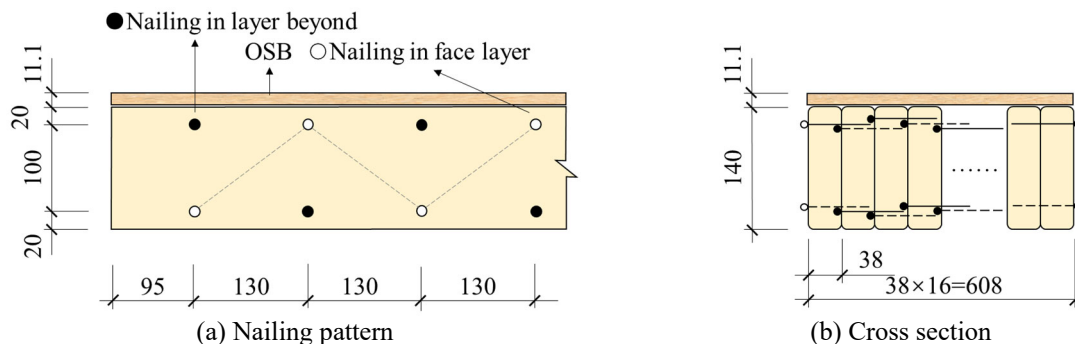


Figure 1: Configuration of the NLT specimen

The configuration of the NLT specimens is depicted in Figure 1, which was designed based on *Nail-laminated Timber U.S. Design & Construction Guide* [3]. The laminations used for the NLT specimens are from the same batch as the lamination specimens. 10 replicates were designed for the NLT panel.

The configuration of the NLTCC specimens is depicted in Figure 2. The NLT part in the NLTCC panel has the same section size as the NLT specimen, but with a length of 4270 mm. The concrete topping with the depth of 60 mm is sheathed at the top of the NLT through the 45° inclined STSs. 2 replicates were designed for the NLTCC panel.

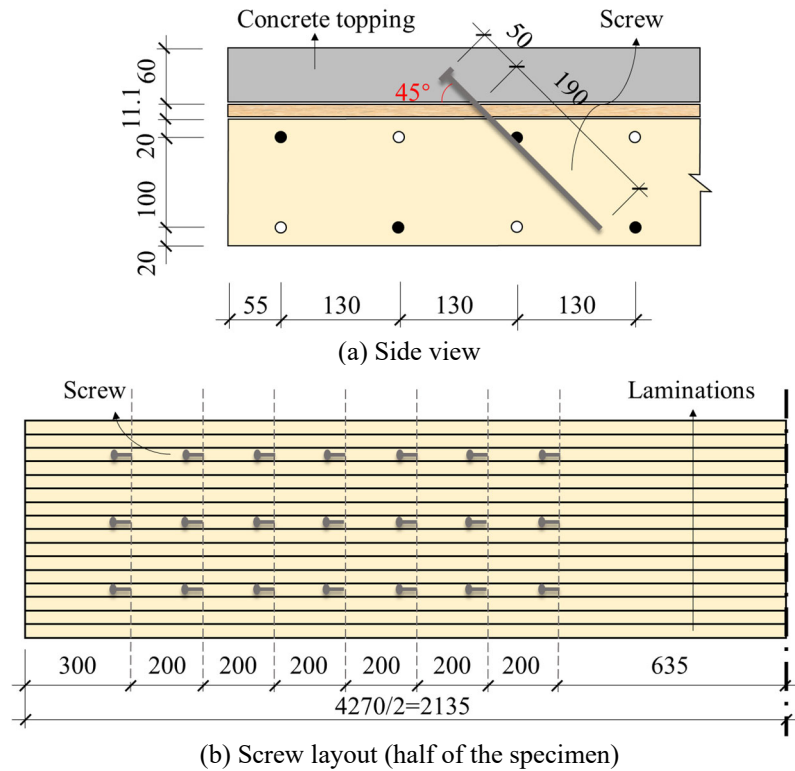


Figure 2: Configuration of the NLTCC specimen

### 2.3. Bending test

Four-point bending tests were conducted based on ASTM D198-15 [12]. As the similar loading approach were used for the lamination, the NLT and the NLTCC panels, Figure 3 only shows the test setup of the NLTCC panel. The net span length for the lamination, the NLT and the NLTCC panel are 2700 mm, 2700 mm, and 3900 mm, respectively. A constant displacement loading rate of 5.0 mm/min was applied to the specimens until failure.

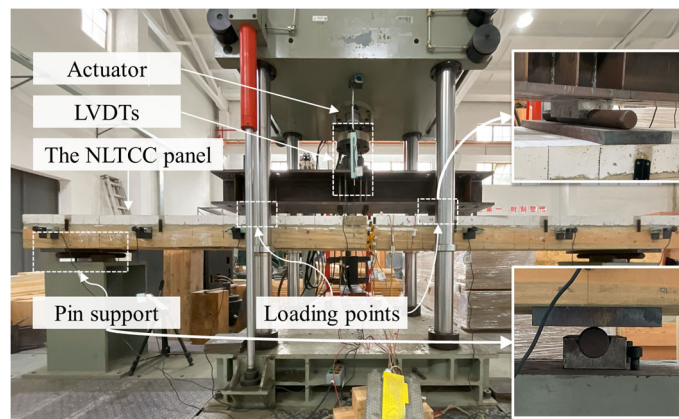


Figure 3: Four-point bending test

### 3. Results and discussion

#### 3.1. Comparison between the NLT and the lamination

The load-deflection curves of the lamination and the NLT are depicted in Figure 4. The laminations exhibited the linear elastic behavior in the initial loading stage. With the deflection increased, a slight descendance of the stiffness was observed. Most of the laminations failed suddenly upon the crack occurred near the wood knots, which was a typical brittle failure.

The NLT also exhibited the linear elastic behavior in the initial loading stage. With the deflection increased, a descendance of load was observed, which was caused by the failure of part of the laminations. The stiffness also had a slight decrease. However, as the remained laminations in the specimen could still carry the increased load, the ultimate load of NLT did not reach at this point. With the successive crack of the laminations, a ladder-type descending load could be observed in the curves. The failure of NLT became more moderate than that of the single lamination.

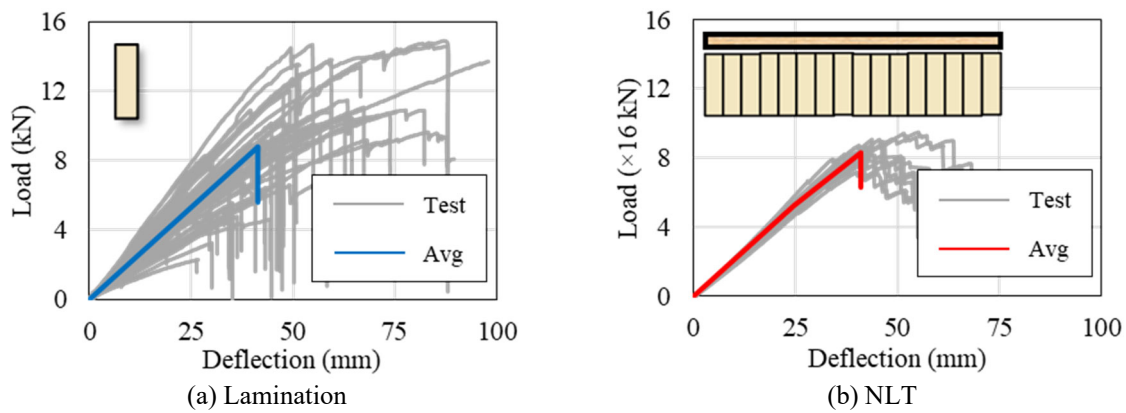


Figure 4: Load-deflection curves

The modulus of elasticity (MOE) of the lamination ( $E_{lam}$ ) and the NLT ( $E_{NLT}$ ) are calculated based on Equations (1) to (2), where  $a$  is the distance between the loading point and the nearest support;  $l$  is the span length;  $F_1$  and  $F_2$  are respectively 10% and 40% of the ultimate load  $F_{max}$ ;  $I$  is the inertial moment of the cross section;  $\omega_1$  and  $\omega_2$  are the global deflection corresponding to  $F_1$  and  $F_2$ , respectively;  $b$  is the width of the cross section and  $h$  is the height of the cross section. The bending strength of the lamination ( $f_{b,lam}$ ) and the NLT ( $f_{b,NLT}$ ) are calculated based on Equation (3). The results are listed in Table 1 and Table 2, where  $f_{b,1}$  is the bending stress of NLT corresponding to the first load-descending point in the curves.

$$E = \frac{a(3l^2 - 4a^2) \cdot (F_2 - F_1)}{48I \cdot (\omega_2 - \omega_1)} \quad (1)$$

$$I = \frac{bh^3}{12} \quad (2)$$

$$f_b = \frac{F_{max} \cdot l}{bh^2} \quad (3)$$

Compared to the lamination, the average MOE and the average strength of the NLT panels do not change significantly. However, there is an obvious reduction in the variability of the bending properties due to the load sharing and the load redistribution effect. For design purpose, the 5th percentile bending strength can be determined with the parameter estimation method. The 5th percentile bending strength of the lamination is 12.6 MPa. For the conservative consideration, the 5th percentile bending strength of the NLT corresponding to the first load-descending point is 18.0 MPa, which is 42.9% higher than that of the lamination, indicating a more reliable bending performance of the NLT.

Table 1: Bending properties of the lamination

No.	$E_{lam}$ (GPa)	$f_{b,lam}$ (MPa)	No.	$E_{lam}$ (GPa)	$f_{b,lam}$ (MPa)	No.	$E_{lam}$ (GPa)	$f_{b,lam}$ (MPa)	No.	$E_{lam}$ (GPa)	$f_{b,lam}$ (MPa)
1	9.77	36.8	14	10.47	29.1	27	6.16	25.5	40	4.55	11.8
2	10.62	38.4	15	7.26	14.5	28	10.34	50.1	41	8.22	40.2
3	8.10	32.0	16	11.47	27.8	29	13.29	53.3	42	9.75	38.0
4	5.97	24.7	17	11.49	49.2	30	6.96	33.3	43	5.73	16.5
5	6.40	20.2	18	9.26	35.0	31	3.67	8.3	44	7.36	22.5
6	7.83	17.9	19	11.01	42.9	32	9.91	33.1	45	9.09	16.7
7	7.59	50.3	20	9.98	41.6	33	8.19	18.1	46	5.34	17.3
8	10.30	53.7	21	9.11	37.2	34	9.38	48.9	47	6.31	20.2
9	13.44	35.9	22	6.81	11.6	35	6.55	21.8	48	11.50	53.0
10	7.90	27.6	23	5.58	16.9	36	9.73	33.8	49	8.68	37.0
11	8.02	38.3	24	7.57	39.2	37	8.34	34.8	50	7.94	18.8
12	8.57	39.2	25	7.23	33.4	38	7.74	24.4	<b>Avg</b>	<b>8.54</b>	<b>31.9</b>
13	9.36	41.7	26	9.36	39.6	39	11.95	43.6	<b>COV</b>	<b>25.0%</b>	<b>38.4%</b>

Table 2: Bending properties of the NLT

No.	$E_{NLT}$ (GPa)	$f_{b,1}$ (MPa)	$f_{b,NLT}$ (MPa)	No.	$E_{NLT}$ (GPa)	$f_{b,1}$ (MPa)	$f_{b,NLT}$ (MPa)
1	8.20	23.0	29.5	7	9.71	24.2	34.4
2	8.79	21.3	29.5	8	8.32	24.9	27.6
3	9.07	29.0	32.9	9	9.26	22.2	32.9
4	7.61	17.7	26.4	10	8.63	26.8	29.6
5	7.76	23.2	28.5	<b>Avg</b>	<b>8.57</b>	<b>23.3</b>	<b>30.5</b>
6	8.38	20.3	33.3	<b>COV</b>	<b>7.7%</b>	<b>13.8%</b>	<b>8.9%</b>

### 3.3. Comparison between the NLTCC and the NLT panels

The moment-rotation curves of the NLTCC and the NLT panels are depicted in Figure 5a. The NLTCC panel exhibited the linear elastic behavior in the initial loading stage. With the deflection increased, cracks first occurred in the concrete near the loading points. A descendance of load was also observed due to the failure of the laminations. The stiffness also had a slight decrease. The specimens could still carry the increased load with the remained laminations. Then, cracks in the concrete appeared in the midspan. The ultimate load of the NLTCC panel reached after the failure of several laminations. The failure of the NLTCC panel was dominated by the failure of the NLT.

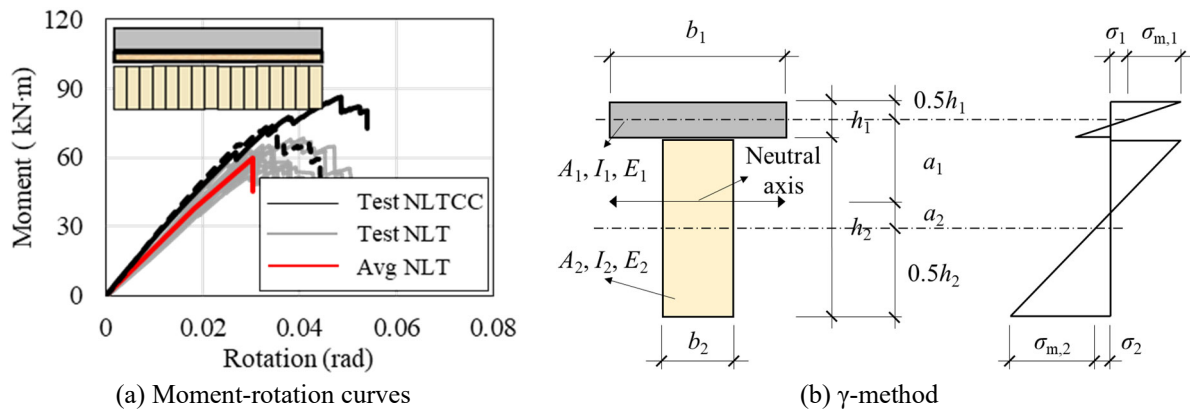


Figure 5: Comparison between the NLTCC and the NLT panels

Based on Equations (4) to (5), the effective bending stiffness of the NLTCC panels ( $EI_{eff,com}$ ) and the MRC of the NLTCC panels ( $M_{b,com}$ ) can be calculated. The results are listed in Table 3, where  $M_{b,com,1}$

is the moment corresponding to the first load-descending point. The effective bending stiffness of NLT ( $EI_{\text{eff,NLT}}$ ) and the MRC of NLT ( $M_{\text{b,NLT}}$ ) can also be calculated for the comparison with the NLTCC panels. The average  $EI_{\text{eff,NLT}}$  is 1190 kN·m. The average MRC of NLT corresponding to the first load-descending point is 46.2 kN·m and the average  $M_{\text{b,NLT}}$  is 60.5 kN·m. Due to the partial composite action, the bending performance of the NLTCC panel is greatly enhanced compared to the NLT panel. Compared to the NLT panel, the average bending stiffness of the NLTCC panels improves by 78.2%. For a conservative consideration, the MRCs corresponding to the first load-descending point are compared. The average MRC of the NLTCC panels improves by 38.3%.

$$EI_{\text{eff,com}} = \frac{a(3l^2 - 4a^2) \cdot (F_2 - F_1)}{48(\omega_2 - \omega_1)} \quad (4)$$

$$M_{\text{b,com}} = \frac{F_{\text{max}} a}{2} \quad (5)$$

Table 3: Bending properties of the NLTCC panels

No.	$EI_{\text{eff,com}}$ (kN·m)	$M_{\text{b,com,1}}$ (kN·m)	$M_{\text{b,com}}$ (kN·m)
1	2050	62.3	86.3
2	2190	65.5	73.2
<b>Avg</b>	<b>2120</b>	<b>63.9</b>	<b>79.8</b>

$\gamma$ -method [13] was employed to predict the bending performance of the NLTCC panel. The typical cross section and the stress distribution can be simplified as Figure 5b.  $E_1$  is determined as 28000 MPa based on [11], while the other values are consistent with those in the tests. The predicted effective bending stiffness can be calculated using Equations (6) to (9), where  $s_i$  is the screw spacing;  $K_i$  is the slip modulus of the screw, which is 7.6 kN/mm according to the push-out test results. The  $EI_{\text{eff},\gamma}$  is calculated as 2020 kN·m, which is 4.7% lower than the tested results.

$$EI_{\text{eff},\gamma} = \sum_{i=1}^2 (E_i I_i + \gamma_i E_i A_i a_i^2) \quad (6)$$

$$\gamma_1 = [1 + \pi^2 E_i A_i s_i / (K_i l^2)]^{-1} \quad (7)$$

$$\gamma_2 = 1 \quad (8)$$

$$a_2 = \frac{\gamma_1 E_1 A_1 (h_1 + h_2)}{2 \sum_{i=1}^2 \gamma_i E_i A_i} \quad (9)$$

The predicted MRC can be calculated based on Equations (10) to (11). Based on the bending test, although concrete cracks appeared prior to the NLT, the steel bars embedded in the concrete could still resist the tension stress induced by bending. Therefore, the first MRC descendance was caused by the crack of the laminations. Therefore, it is assumed that the MRC of the NLTCC panel is reached when the tensile stress in the NLT part reaches its average bending strength, i.e.,  $\sigma_{m,2} + \sigma_2 = f_{b,1}$ . The predicted  $M_{\text{b,com,1}}$  is equal to 72.3 kN·m, which is 11.3% higher than the tested results.

$$\sigma_i = \frac{\gamma_i E_i a_i M}{EI_{\text{eff},\gamma}} \quad (10)$$

$$\sigma_{m,i} = \frac{0.5 E_i h_i M}{EI_{\text{eff},\gamma}} \quad (11)$$

## 5. Conclusion

Based on the bending tests of the lamination, the NLT and the NLTCC panels, the main conclusions can be drawn as follows.

- (1) The average MOE and the average bending strength of NLT do not change obviously compared to those of the lamination. However, there is a reduction in the variability of these bending properties. The 5th percentile bending strength of NLT could be 42.9% higher than that of the lamination, indicating a more reliable bending performance of NLT.
- (2) The effective bending stiffness and the MRC of the NLTCC panels can improve by 78.2% and 38.3% respectively compared to those of the NLT.  $\gamma$ -method could reasonably predict the bending performance of the NLTCC panels, with an underestimation by 4.7% for the bending stiffness and an overestimation by 11.3% for the MRC.

## Acknowledgements

The authors gratefully acknowledge National Natural Science Foundation of China (Grant No. 52078371) and Shanghai Science and Technology Innovation Action Plan Technical Standards Project (Grant No. 23DZ2204200) for supporting this research.

## References

- [1] M. He, F. Lam, H. Xiong, X. Song, S. Zhang, Z. Li, *Timber Engineering, 2nd ed*, Beijing, 2021.
- [2] X. Sun, M. He, Z. Li, "Novel Engineered Wood and Bamboo Composites for Structural Applications: State-of-art of Manufacturing Technology and Mechanical Performance Evaluation," *Construction and Building Materials*, vol. 249, article ID. 118751, 2020.
- [3] Binational Softwood Lumber Council, *Nail-Laminated Timber U.S. Design & Construction Guide v1.0*, Surrey, 2017.
- [4] M. Derikvand, H. Jiao, N. Kotlarewski, M. Lee, A. Chan, G. Nolan, "Bending Performance of Nail-laminated Timber Constructed of Fast-grown Plantation Eucalypt," *European Journal of Wood and Wood Products*, vol. 77, no. 3, pp. 421-437, 2019.
- [5] Z. Li, W. Feng, M. He, F. Chen, X. Sun, "Bending Performance of Nail Laminated Timber: Experimental, Analytical and Numerical Analyses," *Construction and Building Materials*, vol. 389, article ID. 131766, 2023.
- [6] A. Taoum, H. Jiao, D. Holloway, J. Shanks, "Behaviour of Locally Post-tensioned Nail Laminated High Mass Floor Panels under Serviceability Loads," *Australian Journal of Structural Engineering*, vol. 20, no. 2, pp. 115-123, 2019.
- [7] M. Derikvand, N. Kotlarewski, M. Lee, H. Jiao, A. Chan, G. Nolan, "Short-term and Long-term Bending Properties of Nail-laminated Timber Constructed of Fast-grown Plantation Eucalypt," *Construction and Building Materials*, vol. 211, pp. 952-964, 2019.
- [8] E. L. Herberg, "Flexural Performance of Nail-laminated Timber Crane Mats," Master dissertation, University of Minnesota, Twin Cities, Minnesota, 2018.
- [9] K. E. M. Hong, "Structural Performance of Nail-laminated Timber-concrete Composite floors," Master dissertation, University of Waterloo, Waterloo, Ontario, 2017.
- [10] *The Standard for Test Method of Mechanical Properties on Ordinary Concrete*, GB/T 723 50081, 2016.
- [11] *Code for Design of Concrete Structures*, GB 50010, 2015.
- [12] *Standard Test Methods of Static Tests of Lumber in Structural Sizes*, ASTM D198-15, 2015.
- [13] *Eurocode 5: Design of Timber Structures-Part 1-1: General-Common Rules and Rules for Buildings*, BS EN 1995-1-1: 2004, 2004.